

Research Article

Derivation of Single Particle Drying Kinetics of Tapioca Flour

¹Suherman, ²T.K. Berkah Fajar and ¹A. Margaretha Praba

¹Department of Chemical Engineering,

²Department of Mechanical Engineering, University of Diponegoro, Semarang, Indonesia

Abstract: The single particle drying kinetics of powdery tapioca flour has been derived from fluidized bed drying experiments which the inlet gas temperatures is varied (40, 50 and 60°C, respectively). The derivation is performed by scale down method from experiment data uses the FLUBED software which the normalized drying curve is adjusted by iterative method. The FLUBED language programming is developed based on fluidized bed drying model using a two-phase theory. From high moisture content (0.44 kg/kg, wet base) until the product specification i.e., $X_{wb} = 0.14$ (kg/kg) and in three different conditions of the inlet gas temperatures, the application of the normalized drying curve gives an excellent performance of simulation results intend that the normalization method works well. The drying curve has two drying period namely constant drying rate period and falling drying rate period, where X_{cr} is 0.35.

Keywords: Drying, fluid bed, modeling, tapioca

INTRODUCTION

In the production of tapioca flour, the drying process is attended to reduce moisture content in starch from 40 to 14% (wet bases). Normally, in Small Medium Enterprises (SME) of tapioca flour in District Pati, Central Java, Indonesia the drying process is done by dried under the sun on the open floor. The drying process is performed conventionally by spreading flour on drying floor under sunlight and takes a minimum of 6 h. Furthermore, when overcast or going to rain, the process production of tapioca flour is stopped. Besides that, by this drying method quality of the product away from the SNI (Indonesia Standard) standard. Therefore, in this study was developed a simulated continuous dryer for drying of tapioca flour by scaling-up from batch experimental data.

Problems encountered in drying of starch are in a state of great water vapor, some fraction of starch agglomerated into large particles. The size of tapioca starch is in the powdery form, then it is included in the category of Geldart Group C where the material is cohesive. In addition the moisture contained materials is bound moisture (Perdomo *et al.*, 2009). Starch fractions have undesirable functional properties such as low viscosity, high gelatinization temperature and the rate of hydrolysis of acid/low enzyme (Tang *et al.*, 2001; Liu *et al.*, 2009). In addition, the particles can cause a problem in the handling of such during the transport or drying (Boonyai *et al.*, 2004; Turchiuli *et al.*, 2005). Starch fraction will be reprocessed, so that production costs are higher. Furthermore

Aichayawanicha *et al.* (2011), conducted research on the phenomenon of agglomeration of tapioca flour in pneumatic drying. It was found that the phase transition of starch correlated with agglomeration during drying. When phase of starch in rubbery phase, agglomeration of starch particle increases. However, agglomeration of starch decreased as the starch in the glassy phase. This suggests that the mechanism of agglomeration of starch is the result of the formation of both solid and liquid bridges (Foster *et al.*, 2006; Tomas, 2007). Agglomeration also occurs when there is a collision between particles (Truong *et al.*, 2004). In order to reduce agglomeration of starch due liquid bridge formation during the drying process, the starch must be dried at a lower temperature than the glass transition temperature. Meanwhile, the starch suspension was dried in spouted bed with inert particles (Pereira *et al.*, 2010). Furthermore, this study intended studied in the derivation of single particle drying kinetics of tapioca flour.

To be able to design an optimal drier, the drying kinetics curves of the single particles of the solid product is must be known (Suherman and Tsotas, 2006). From this single particle drying curves can be scale-up in a variety of types and dimensions of the dryer. Drying curve can only be known through experimental measurements. For granular products, drying curve of single particle simply can be directly measured by differential method. However, if the differential measurement is not possible, then the drying curve can be derived by measuring the drying integral multiple particles simultaneously. This last

method is usually used for powdery products. Further integral drying curve is extracted into a single particle drying curve by scale-down method. Process scale-up and scale-down requires a model that calculates the drying curve integral and single particle simultaneously. The fluidized bed dryer models that have been developed based on two-phase models (bubble and suspension phase) and the concept of normalized drying curve (Suherman and Tsotas, 2008), here in after referred to as FLUBED (Suherman, 2007). In this study, the discussion more thoroughly about the derivation of single normalized drying curve of tapioca flour from batch fluidized bed drying data.

EXPERIMENTS AND MODELING METHOD

Experiments method: Figure 1 shows the apparatus set-up. The wet tapioca flour was taken from SMEs Tapioca Starch in Sidomukti, Pati, Central Java, Indonesia. The diameter of bed is 150 mm. The humidity and flow rate of inlet air is 18.24 g/kg and 25 m³/h, respectively. The initial mass and moisture content of wet solid is 0.2 kg and 0.44 kg/kg (wb), respectively. The particle diameter and density of tapioca is 16.6 μm and 1114 kg/m³. Inlet air temperature (T_{gi}) is varied namely 40, 50 and 60°C, respectively. The process starts with an experiment that will turn on the blower air flow dryer. Furthermore, air heaters be positioned as desired, e.g., 50°C. After drying air temperature reaches the temperature desired, tapioca starch material is inserted into the bed. Finally, the drying process is conducted for 30 min. The temperature controller TIC (below distributor) maintains inlet air temperature at the desired level. During the experiment, inlet air temperature, outlet air temperature and outlet air humidity is measured each 1 min. At the end of the experiment, samples were taken for the starch solids are then measured the water vapor content using the oven method:

The solid moisture content is calculated by:

$$X(t) = X_0 - \frac{\dot{M}_g}{M_{s,dry}} \int_{t=0}^t (Y_{out}(t) - Y_{in}(t)) dt \quad (1)$$

where,

- X₀ = Initial moisture content
- M_g = Air mass flow rate
- M_{s,dry} = Dry mass of particle
- Y = Air humidity

And drying rate is calculated by:

$$\dot{m} = \frac{\dot{M}_g}{M_{s,dry}} \frac{\rho_p d_p}{6} (Y_{out}(t) - Y_{in}) \quad (2)$$

where,

- ρ_p = Particle density
- d_p = Particle diameter

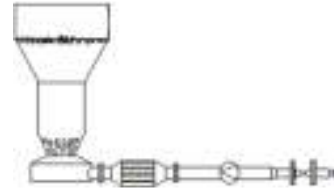


Fig. 1: Apparatus set-up

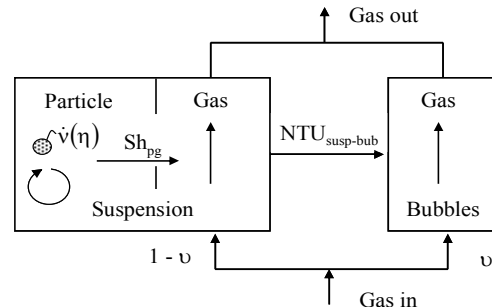


Fig. 2: Schematic of two phase fluid bed drying model

Modeling: Modeling of fluidized bed drying using a two-phase theory has been introduced by Tsotsas (Groenewold and Tsotsas, 2007) which can be described schematically as in Fig. 2. The theory is based on two phases the following assumptions:

- Perfect back particles mixing
- The bubble phase and the suspension phase
- The mass transfer between bubble and suspension phases (active bypass)

The next three parameters to be calculated, namely:

- Sherwood number Sh_{pg} to calculate mass transfer between particles and gas suspension
- Number of transfer units NTU_{susp-bub} to calculate mass transfer between the bubble phase and the suspension
- Bubble flow rate υ

According to Fig. 2, the total mass balance for the particles can be derived:

$$M_{s,dry} \frac{dX}{dt} = - \int_0^L \dot{M}_{p-susp} d\zeta \quad (3)$$

where,

- M_{s,dry} : Dry mass of the particle
- M_{p-susp} : The mass flow rate of particles to the suspension phase

Variable ζ is height non-dimensional coordinates are defined as:

$$\zeta = z/L_{bed} \quad (4)$$

Mass balance between the suspension and the bubble phase:

$$(1 - \upsilon)\dot{M}_g \frac{dY_{susp}}{d\zeta} = \dot{M}_{p-susp} - \dot{M}_{susp-bub} \quad (5)$$

$$\upsilon\dot{M}_g \frac{dY_{bub}}{d\zeta} = \dot{M}_{susp-bub} \quad (6)$$

Kinetics of particle-suspension and suspension-bubble:

$$\dot{M}_{p-susp} = \dot{m}/A_{p-susp} \quad (7)$$

$$\dot{m} = \dot{v}(\eta)\rho_g\beta_g(Y^*(T_{AS}) - Y) \quad (8)$$

$$\dot{M}_{susp-bub} = \rho_g\beta_{susp-bub}A_{susp-bub}(Y_{susp} - Y_{bub}) \quad (9)$$

where,

A_{p-susp} = The area of the particles to the gas suspension (total area of particles)

\dot{M}_{p-susp} = The mass flow rate of the gas particle suspensions

The ratio of bubble to the total gas flow rate, υ , can be calculated according to Hillgardt and Werther for different Geldart Group:

$$\upsilon = \upsilon_r \frac{Re_0 - Re_{mf}}{Re_0} \quad (10)$$

where, Re_0 and Re_{mf} is Reynolds Numbers on superficial velocity and minimum fluidization.

Dimensionless numbers bubble flow rate that can be observed, υ_r , derived from:

Group A:

$$\upsilon_r = 0.8, \quad (11)$$

Group B:

$$\upsilon_r = \begin{cases} 0.67 & \text{if } \frac{L_{bed}}{d_{bed}} < 1.7 \\ 0.384 \frac{d_{bed}}{L_{bed}} + 0.34 \sqrt{\frac{L_{bed}}{d_{bed}}} & \text{if } 1.7 \leq \frac{L_{bed}}{d_{bed}} < 4.0 \\ 1 - 0.8946 \frac{d_{bed}}{L_{bed}} & \text{if } \frac{L_{bed}}{d_{bed}} \geq 4.0 \end{cases} \quad (12)$$

Group D:

$$\upsilon_r = \begin{cases} 0.26 & \text{if } \frac{L_{bed}}{d_{bed}} < 0.55 \\ 0.0478 \frac{d_{bed}}{L_{bed}} + 0.2333 \sqrt{\frac{L_{bed}}{d_{bed}}} & \text{if } 0.55 \leq \frac{L_{bed}}{d_{bed}} < 8.0 \\ 1 - 2.6724 \frac{d_{bed}}{L_{bed}} & \text{if } \frac{L_{bed}}{d_{bed}} \geq 8.0 \end{cases} \quad (13)$$

Definition Group based particle diameter d_p in meters and density in kg/m^3 :

Group A:

$$[\rho_{p,dry}(1 + X) - \rho_g] > |66.98d_p - 0.000768|^{-1}, \text{ or } : d_p > 15 \times 10^{-6} \text{ m} \quad (14)$$

Group B:

$$[\rho_{p,dry}(1 + X) - \rho_g]d_p > 0.225 \quad (15)$$

Group D:

$$[\rho_{p,dry}(1 + X) - \rho_g]d_p^2 > 10^{-3} \quad (16)$$

Sherwood number Sh_{pg} calculated use model was developed by Groenewold and Tsotsas (2007):

$$Sh_{pg} = \frac{Re_0 Sc}{A_{p-susp}/F_{bed}} \ln \left(1 + \frac{Sh_{Gnic} A_{p-susp}/F_{bed}}{Re_0 Sc} \right) \quad (17)$$

where,

Sc = Schmidt number

F_{bed} = The cross-sectional area of the bed

Furthermore other parameter was calculated using:

$$Sc = \nu_g / \delta_g \quad (18)$$

$$Re_0 = u_0 d_p / \nu_g \quad (19)$$

$$u_0 = \dot{M}_g / (\rho_g F_{bed}) \quad (20)$$

$$\frac{A_{p-susp}}{F_{bed}} = 6(1 - \epsilon) \frac{L_{bed}}{d_p} \quad (21)$$

$$L_{bed} = \frac{M_{s,dry}}{\rho_{p,dry} F_{bed} (1 - \epsilon)} \quad (22)$$

$$\beta_g = Sh_{p-susp} \delta_g / d_p \quad (23)$$

$$NTU_{p-susp} = \frac{Sh_{p-susp} A_{p-susp}/F_{bed}}{Re_0 Sc} \quad (24)$$

where ν_g is kinematic viscosity.

Bed expansion is calculated by:

$$\epsilon = (Re_0 / Re_{clu})^{1/b} \quad (25)$$

$$b = \frac{\ln(Re_{mf}/Re_{clu})}{\ln \epsilon_{mf}} \quad (26)$$

$$Re_{mf} = 42.9(1 - \epsilon_{mf}) \left\{ \sqrt{1 + \frac{\epsilon_{mf}^3 Ar}{(1 - \epsilon_{mf})^2 3214}} - 1 \right\} \quad (27)$$

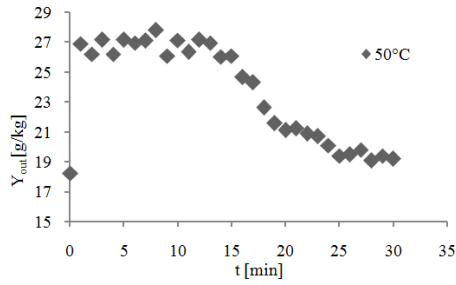


Fig. 3: Typical measurement result of drying of tapioca flour in fluidized bed; humidity of outlet gas

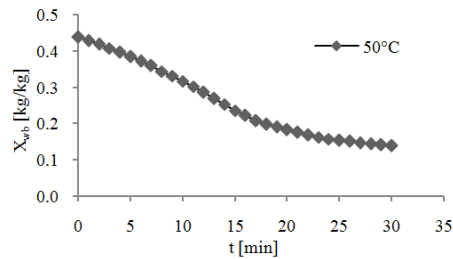


Fig. 4: Typical measurement result of drying of tapioca flour in fluidized bed; solid moisture content

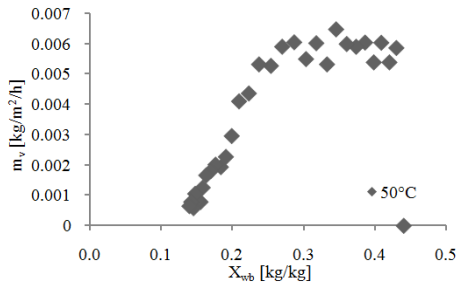


Fig. 5: Typical measurement result of drying of tapioca flour in fluidized bed; drying rate

$$Re_{elu} = \sqrt{4Ar/3} \quad (28)$$

$$Ar = \frac{gd_p^3}{v_g^2} \cdot \frac{\rho_{p,dry}(1+X) - \rho_g}{\rho_g} \quad (29)$$

where,

Re_{elu} = Reynold number at elutriation

Ar = Archimedes number

Numbers transfer unit of gas suspension to bubble phase $NTU_{susp-bub}$ can be calculated by:

$$NTU_{susp-bub} = \frac{\rho_g \beta_{susp-bub} A_{susp-bub}}{M_g} = \frac{L_{bed}}{0.05m} \quad (30)$$

Furthermore, the above model equation can be solved analytically and then be made programming language in MS Excel. This MS Excel programming language then is called as FLUBED.

RESULTS AND DISCUSSION

Experimental results: A typical experimental result is represented in the Fig. 3 to 5. Figure 3 shows the humidity of outlet gas. Starting from at time of approx. 15 min, the humidity of outlet gas drops strongly and leads to a flatter process of the solid moisture content in the Fig. 4. It is followed by the decrease of drying rate in the Fig. 5. The drying rates in the third diagram are calculated from the difference between inlet and outlet of the gas humidity and then multiply by gas mass flow rate Eq. (2). The drying process is considered as terminated for 30 min. The solid moisture content is calculated by indirect method i.e., the evaporation mass flow of water in gas phase Eq. (1). To ensure these results, the solid moisture content of samples at both the beginning and the end of the drying process are measured again by oven drying. Therefore, the water mass balance and the gas mass flow rate always becomes very exactly.

Moreover, within the range mentioned the results of measurement show the drying behavior of the entire fluidized bed. Either the critical moisture content or the drying rate of the single particles in the first and second drying periods are not directly readable from the results of measurement. However, the single particle behavior can be derived by means of normalization. The normalization of drying curve cannot be made directly from these experimental results, but by scale down method using fluidized bed model. The fluidized bed model has been described in section modelling. In scale down process, the developed software FLUBED was used. By the adjustment of the a freely selectable drying curve of the single particle as well as the definition of the critical moisture content, the program computes the drying process of entire solid moisture content in the fluidized bed. The derivation of the normalized drying curve can be adapted by the qualitative and quantitative comparison between the measured and computed of outlet gas humidity as well as the drying rate to a good agreement, which was obtained in an iterative method. In this way, the normalized drying curve from the experiments data can be determined.

Figure 6 to 7 shows experimental result in the different of air temperature. Figure 6 shows by increasing air temperature, the solid moisture content becomes steeper and also the residual solid moisture content becomes lower. It is followed by increasing of drying rate in Fig. 7. In addition, it is also clear that the drying of tapioca flour has two drying period namely constant drying rate period and falling drying rate period.

Derivation of single particle drying curve: The normalized drying curves of the single particles as well as the critical moisture content are derived from measurement results by iterative adjustment in the software FLUBED. For all measurements will give only one normalized drying curve as well as critical moisture content. This result is summarized in Table 1. In the

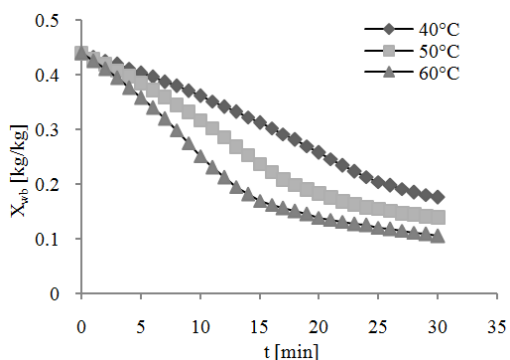


Fig. 6: Measurement result of drying of tapioca flour in fluidized bed; the influence of air temperature on solid moisture content

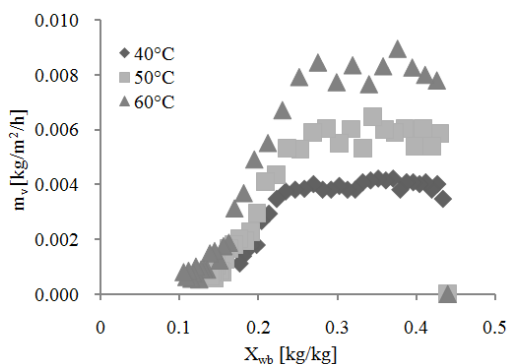


Fig. 7: Measurement result of drying of tapioca flour in fluidized bed; the influence of air temperature on drying rate

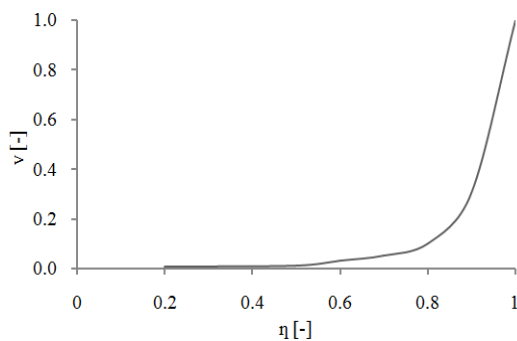


Fig. 8: Normalized drying curve of tapioca flour where X_{cr} is 0.35

application, between the fixed corner points of the normalized drying curve is to be interpolated by linear interpolation. The normalized drying curves are graphically represented in Fig. 8.

The measured and the simulated both residual solid moisture content and drying rate based on the normalized drying curve of tapioca drying in fluidized bed are represented in Fig. 9 and 10. Both residual

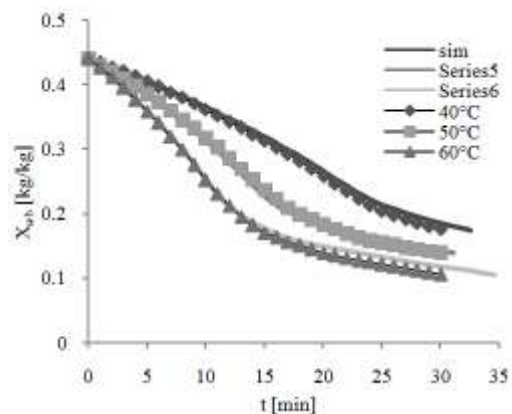


Fig. 9: The influence of temperatures on the measured and simulated residual solid moisture content of tapioca flour drying in fluidized bed

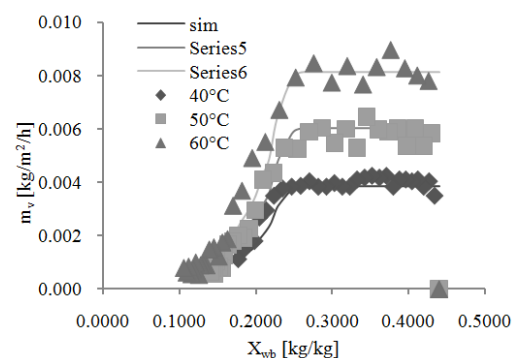


Fig. 10: The influence of temperatures on the measured and simulated drying rate of tapioca flour drying in fluidized bed

Table 1: Normalized drying curve of tapioca flour where X_{cr} is 0.35

η	0.20	0.50	0.60	0.70	0.80	0.90	1
\dot{v}	0.005	0.010	0.03	0.05	0.10	0.30	1

solid moisture content and drying rate curve gives a good agreement between measurement and simulated results. In this diagram, the inlet gas temperatures as parameter in order to illustrate their influence on the drying process.

This also applies in particular to the influence of the temperature. Due to the normalized drying curve is independent to the outside conditions, the excellent performance of results intend that the normalization method works well. The change of the drying rate which causes a variation of the temperature toward end of the drying process is proportional to the change of the drying rate which takes place at same variation of the gas temperature in the first drying period. From measurements use fluidized bed drying, the normalized drying curve can be derived for the whole region of moisture content up to product specification i.e., $X_{wb} = 0.14$.

CONCLUSION

The single particle drying kinetics of powdery tapioca was derived successfully from fluidized bed drying experiments. The drying curve of tapioca has two drying period namely constant drying rate period and falling drying rate period, where X_{cr} is 0.35. The change of the drying rate which causes a variation of the temperature toward end of the drying process is proportional to the change of the drying rate which takes place at same variation of the gas temperature in the first drying period.

ACKNOWLEDGMENT

This study was supported by Directorate Higher Education, Ministry of Education of Republic of Indonesia in the program National Strategic Research No. 008/SP2H/PL/Dit.Litabmas/III/2012.

REFERENCES

- Aichayawanicha, S., M. Nopharatanaa, A. Nopharatanab and W. Songkasiric, 2011. Agglomeration mechanisms of cassava starch during pneumatic conveying drying. *Carbohydrate Polym.*, 84: 292-298.
- Boonyai, P., B. Bhandari and T. Howes, 2004. Stickiness measurement techniques for food powders: A review. *Powder Technol.*, 145: 34-46
- Foster, K.D., J.E. Bronlund and A.H.J. Pasterson, 2006. Glass transition related cohesion of amorphous sugar powders. *J. Food Eng.*, 77: 997-1006.
- Groenewold, H. and E. Tsotsas, 2007. Drying in fluidized beds with immersed heating elements. *Chem. Eng. Sci.*, 62: 481-502.
- Liu, D., Q. Wu, H. Chen and P.R. Chang, 2009. Transitional properties of starch colloid with particle size reduction from micro-to nanometer. *J. Colloid Interf. Sci.*, 339(1): 117-124.
- Perdomo, J., A. Cova, A.J. Sandoval, L. García, E. Laredo and A.J. Müller, 2009. Glass transition temperatures and water sorption isotherms of cassava starch. *Carbohydrate Poly.*, 76: 305-313.
- Pereira, N.R., F.C. Godoi and S.C.S. Rocha, 2010. Drying of starch suspension in spouted bed with inert particles: Physical and thermal analysis of product. *Drying Technol.*, 11: 1288-1296.
- Suherman, 2007. *Drying Kinetics of Granular and Powdery Polymers*. Docupoint Verlag, Magdeburg, Germany, ISBN: 978-3-939665-63-2.
- Suherman, P.M. and E. dan Tsotsas, 2006. Drying kinetics of granular and powdery polymers. *Proceeding of 15th International Drying Symposium, Budapest, Hungary, August 20-23*, pp: 1867-1874.
- Suherman, M.P. and E. Tsotas, 2008. On the applicability of normalization drying kinetics. *Drying Technol Int. J.*, 26(1).
- Tang, H., H. Ando, K. Watanabe, Y. Takeda and T. Mitsunaga, 2001. Physicochemical properties and structure of large, medium and small granules starches in fractions of normal barley endosperm. *Carbohydrate Res.*, 330: 241-248.
- Tomas, J., 2007. Adhesion of ultrafine particles: A micromechanical approach. *Chem. Eng. Sci.*, 62: 1997-2010.
- Truong, V., B.R. Bhandari, T. Howes and B. Adhikari, 2004. Glass transition behavior of fructose. *Int. J. Food Sci. Technol.*, 39: 569-578.
- Turchiuli, C., Z. Eloualia, N.E. Mansouri and E. Dumoulin, 2005. Fluidised bed agglomeration: Agglomerates shape and end-use properties. *Powder Technol.*, 157: 168-175.